Structural and biochemical analysis of the dual-specificity Trm10 enzyme from *Thermococcus kodakaraensis* prompts reconsideration of its catalytic mechanism

(SUPPLEMENTARY MATERIAL)

Ranjan Kumar Singh[1,2,a], André Feller[3,a], Martine Roovers[4,a] , Dany Van Elder[3], Lina Wauters[1,2,5], Louis Droogmans[3,b], Wim Versées[1,2,b]

[1] Structural Biology Brussels, Vrije Universiteit Brussel, Pleinlaan 2, 1050 Brussel, Belgium.

[2] VIB-VUB Center For Structural Biology, Pleinlaan 2, 1050 Brussel, Belgium.

[3] Laboratoire de Microbiologie, Université libre de Bruxelles (ULB), 12 Rue des Professeurs Jeener et Brachet, 6041 Gosselies, Belgium.

[4] Institut de Recherches Microbiologiques Jean-Marie Wiame, Avenue E. Gryson 1, 1070 Bruxelles, Belgium.

[5] Department of Cell Biochemistry, University of Groningen, Nijenborgh 7, Groningen 9747 AG, Netherlands.

[a] These authors contributed equally to this work

[b] Joint corresponding authors. Correspondence to: wim.versees@vub.be or ldroogma@ulb.ac.be

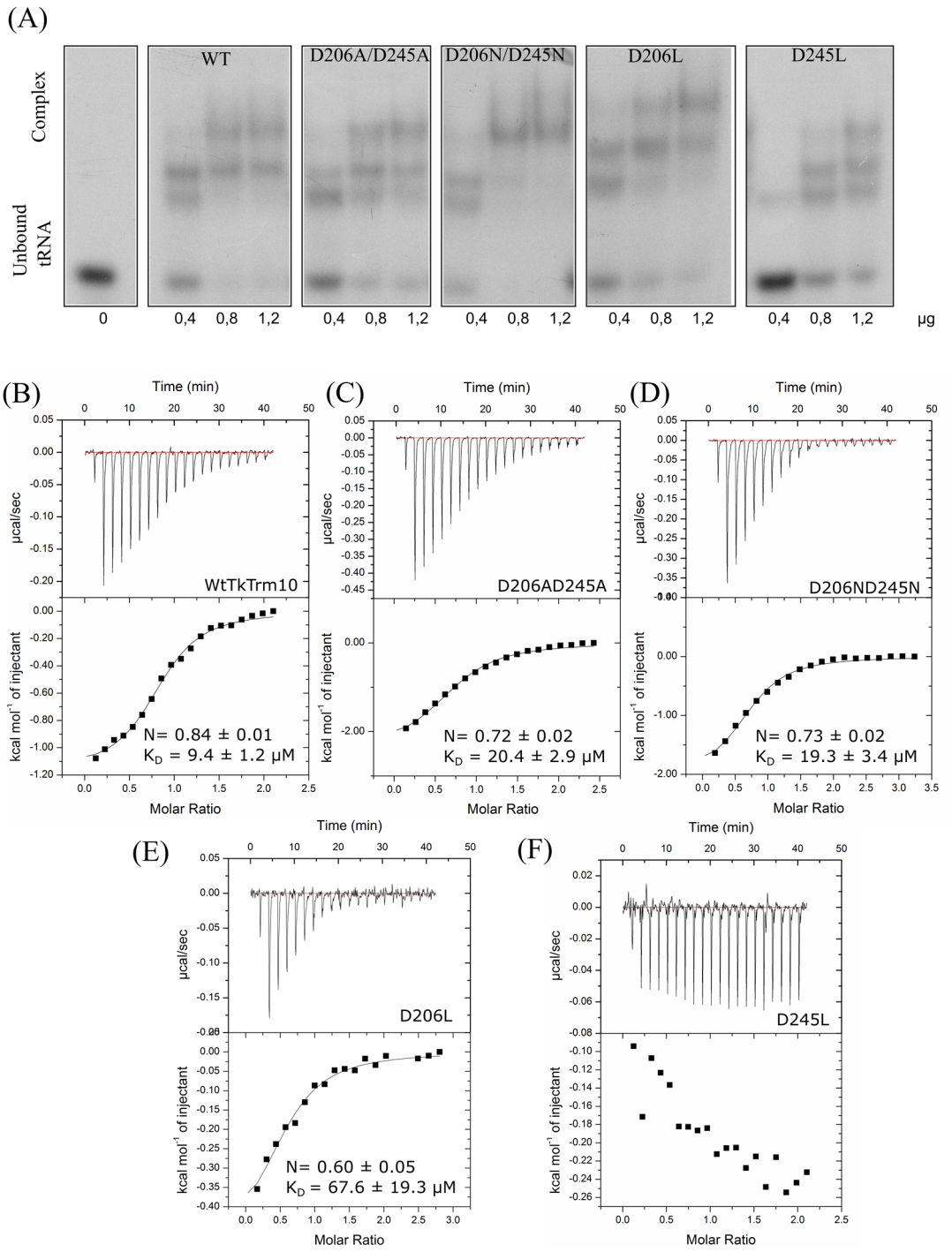

Figure S1: tRNA binding and SAM binding to wild-type and mutant $_{Tk}$Trm10. (**A**) Electrophoretic mobility shift assays (EMSA) showing the binding of $_{Tk}$tRNA^{Asp} on the wild-type, D206A/D245A, D206N/D245N, D206L and D245L $_{Tk}$Trm10 variants. The extreme left panel shows the control experiment in absence of the protein. EMSA for the WT $_{Tk}$Trm10 and the mutants were performed using increasing amounts of enzymes (0.4, 0.8, 1.2 µg). (**B-F**) Isothermal titration calorimetry (ITC) experiments for binding of SAM to wild type $_{Tk}$Trm10 (**B**) and the D206A/D245A (**C**), D206N/D245N **(D)**, D206L (**E**) and D245L (**F**) mutants.

(A)

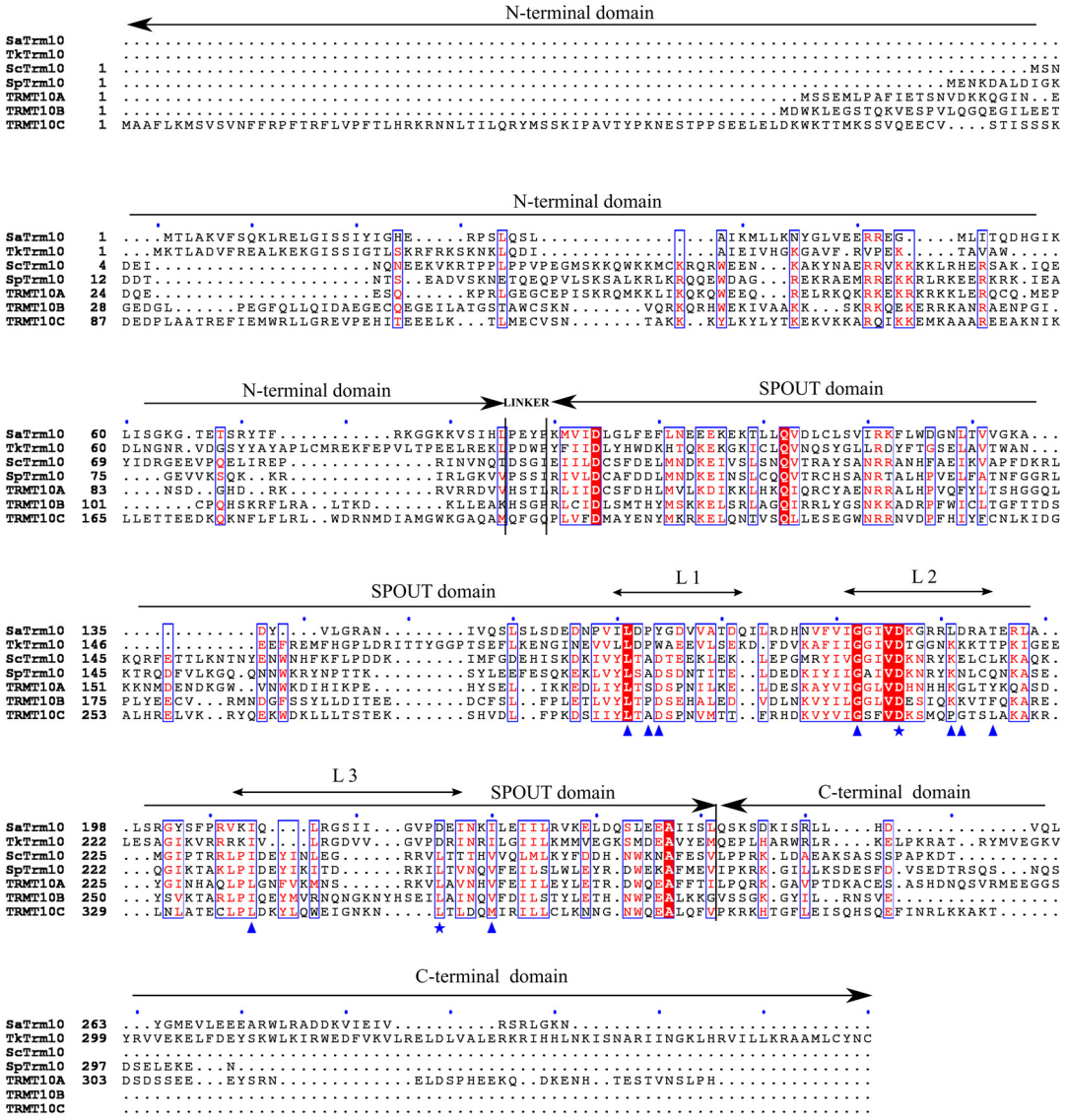

(B)

$_{Tk}$Trm10 (m^1A/m^1G)	$_{Sa}$Trm10 (m^1A)	$_{Sc}$Trm10 (m^1G)	$_{Sp}$Trm10 (m^1G)	TRMT10A (m^1G)	TRMT10B (m^1G)	TRMT10C (m^1A/m^1G)
Gln122	Gln111	Gln118	Gln118	Gln124	Gln148	Gln226
Val205	Val183	Val209	Val206	Val209	Val234	Val313
Asp206	Asp184	Asp210	Asp207	Asp210	Asp235	Asp314
Asp245	Asp220	Leu246	Leu243	Leu246	Leu277	Leu351
Arg246	Glu221	Thr247	Thr244	Ala247	Ala278	Thr352
Arg249	Lys224	His 250	Gln247	His250	Gln281	Gln355
Lys116	Lys105	Ile112	Ile112	Ile118	Leu142	Leu220
Lys118	Lys107	Ser114	Ser114	Lys120	Arg144	Asn222

Figure S2: Sequence alignment and conserved active site residues of Trm10 orthologues. (A) Multiple sequence alignment of Trm10 orthologues. The alignment was performed for archaeal ($_{Sa}$Trm10 and $_{Tk}$Trm10) and eukaryal ($_{Sc}$Trm10 and $_{Sp}$Trm10) Trm10 orthologues discussed in the

manuscript, and for the three human isoforms (TrmT10A, TrmT10B, TrmT10C). Highly conserved residues are highlighted in red. Residues interacting with the cofactor SAM are indicated by blue triangles, residues interacting with both SAM and the incoming nucleobase are indicated by a blue star. (**B**) Numbering of residues discussed in text for the different Trm10 orthologues.

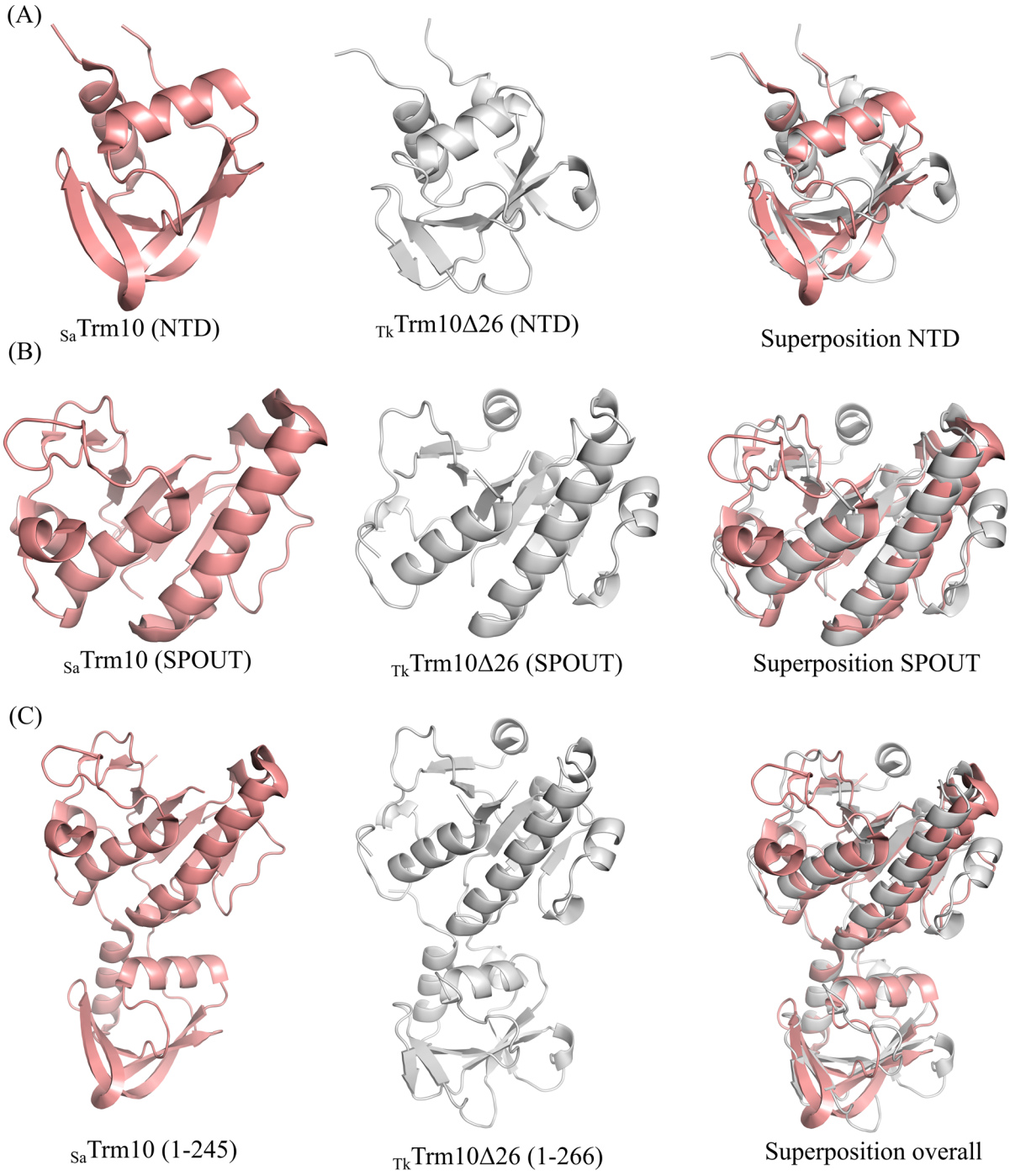

Figure S3. Comparison of $_{Sa}$Trm10 and $_{Tk}$Trm10 structures. Structure and structural superposition of the NTD (**A**), the SPOUT domain (**B**) and the NTD-SPOUT arrangement (**C**) of $_{Sa}$Trm10 (obtained from the $_{Sa}$Trm10_FL structure (PDB ID 5a7y)) and $_{Tk}$Trm10Δ26.

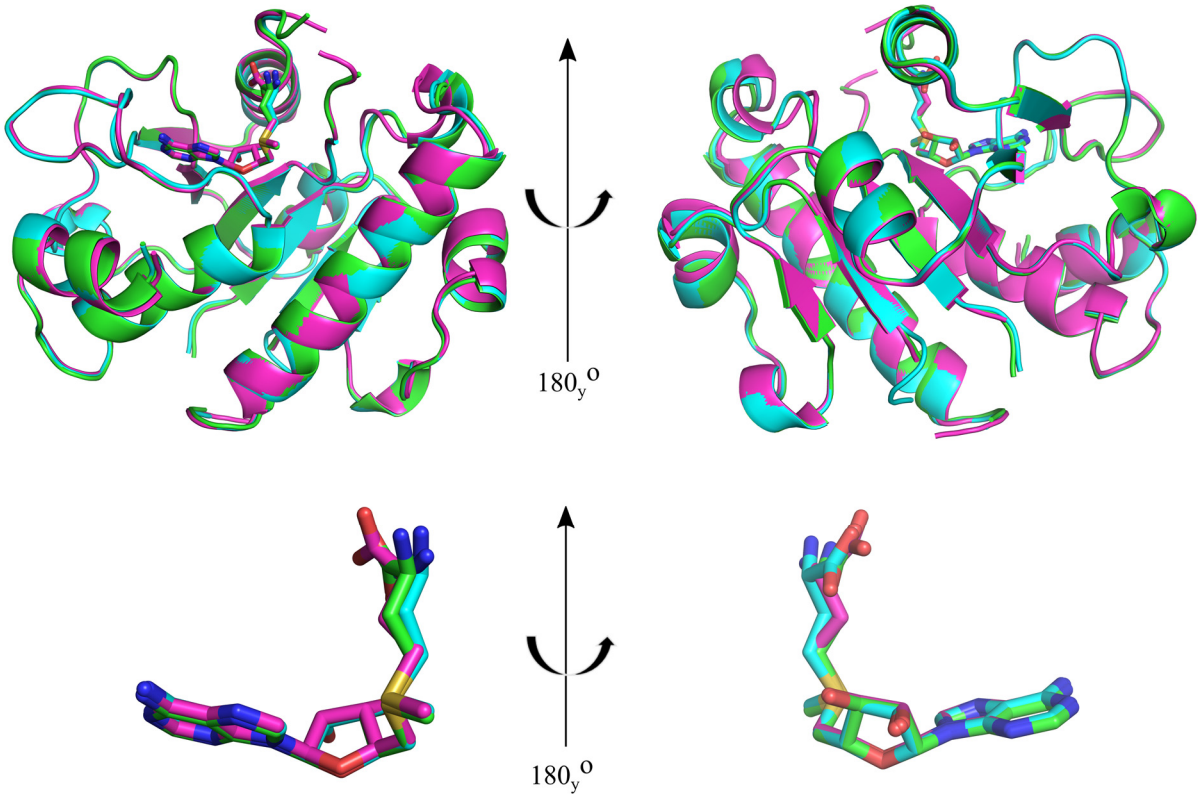

Figure S4. Superposition of the three protein molecules present within the asymmetric unit of the $_{Tk}$SPOUT_SAM crystal structure, shown in two different orientations. The bottom figure shows the superposition of SAM molecules bound to each of the three protein molecules in the asymmetric unit.

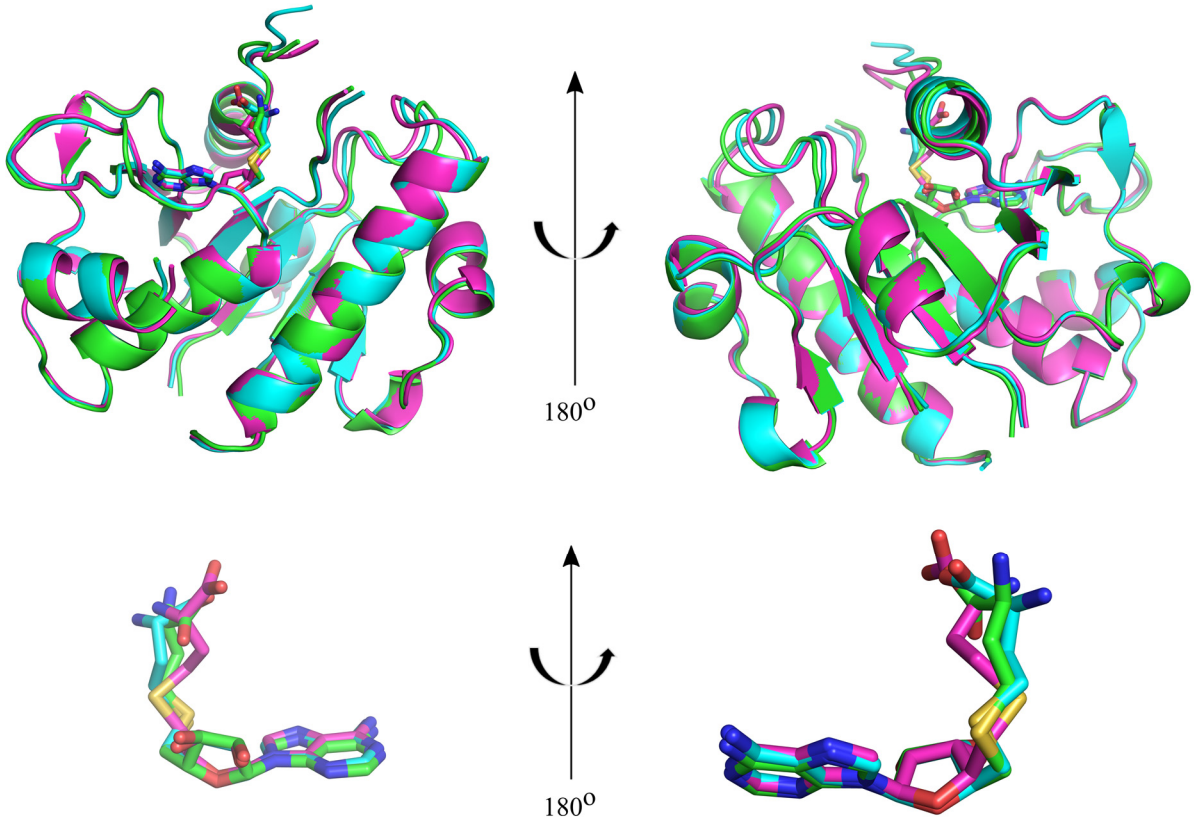

Figure S5. Superposition of the three protein molecules present within the asymmetric unit of the $_{Tk}$SPOUT_SAH crystal structure, shown in two different orientations. The bottom figure shows the superposition of SAH molecules bound to each of the three protein molecules in the asymmetric unit.

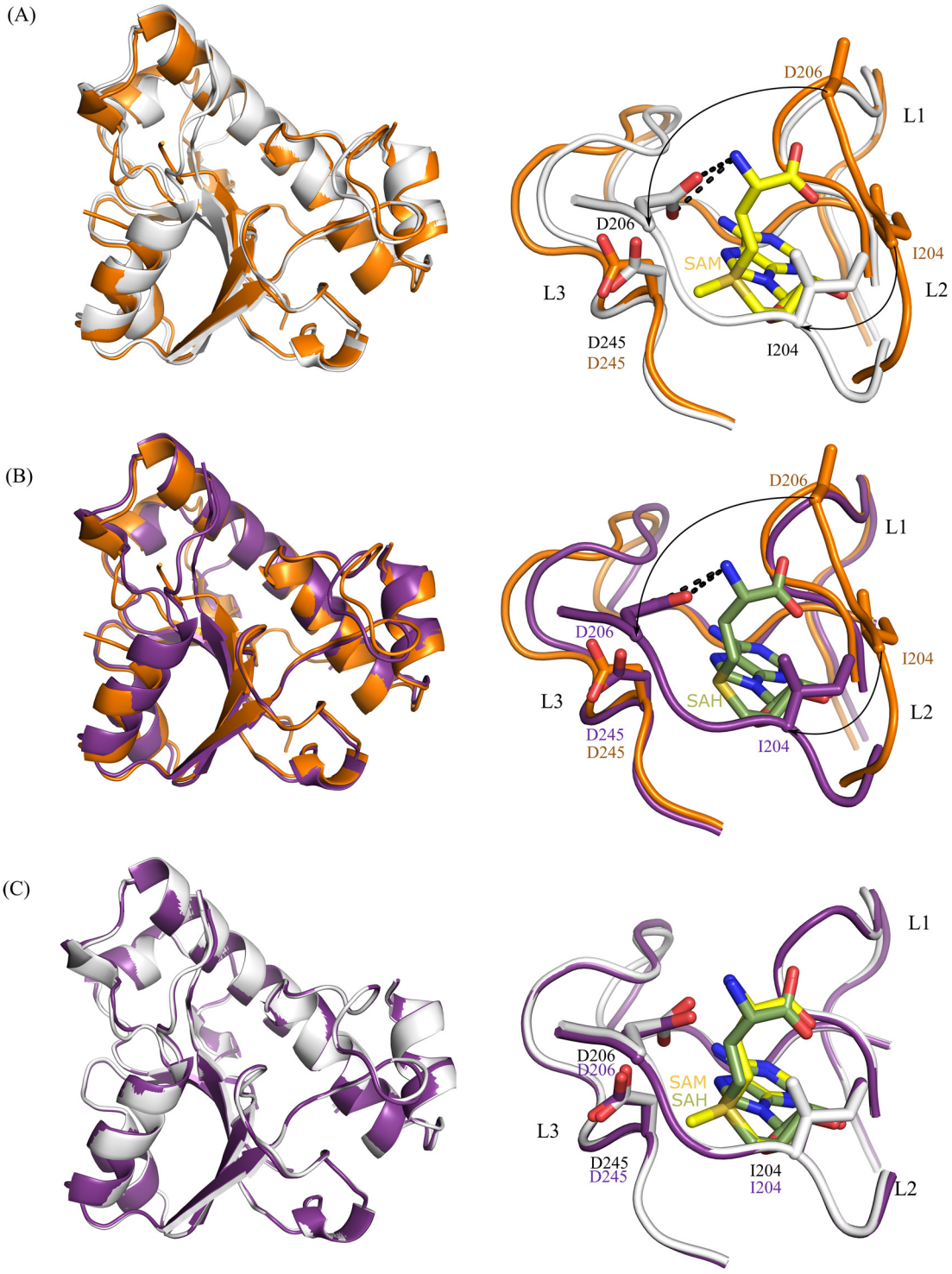

Figure S6. Pairwise superposition of the crystal structures of the SPOUT domain of $_{Tk}$Trm10 in different substrate bound states (APO, SAM-bound, SAH-bound). The left panels show the overall superposition in cartoon representation. The right panels show the conformational changes in the loops of the trefoil knot, and especially in the L2 region. The movement of L2 is shown by curved arrows with reference to the D206 and I204 residues. The SAM and SAH molecules are shown as sticks with carbon

atom colored yellow and green, respectively. (**A**) Superposition of $_{Tk}$SPOUT_SAM (grey) with $_{Tk}$SPOUT_APO (orange). Note that the side chain of D206 is only partially visible in the $_{Tk}$SPOUT_APO structure. (**B**) Superposition of $_{Tk}$SPOUT_SAH (purple) with $_{Tk}$SPOUT_APO (orange). (**C**) Superposition of $_{Tk}$SPOUT_SAH (purple) with $_{Tk}$SPOUT_SAM (grey).

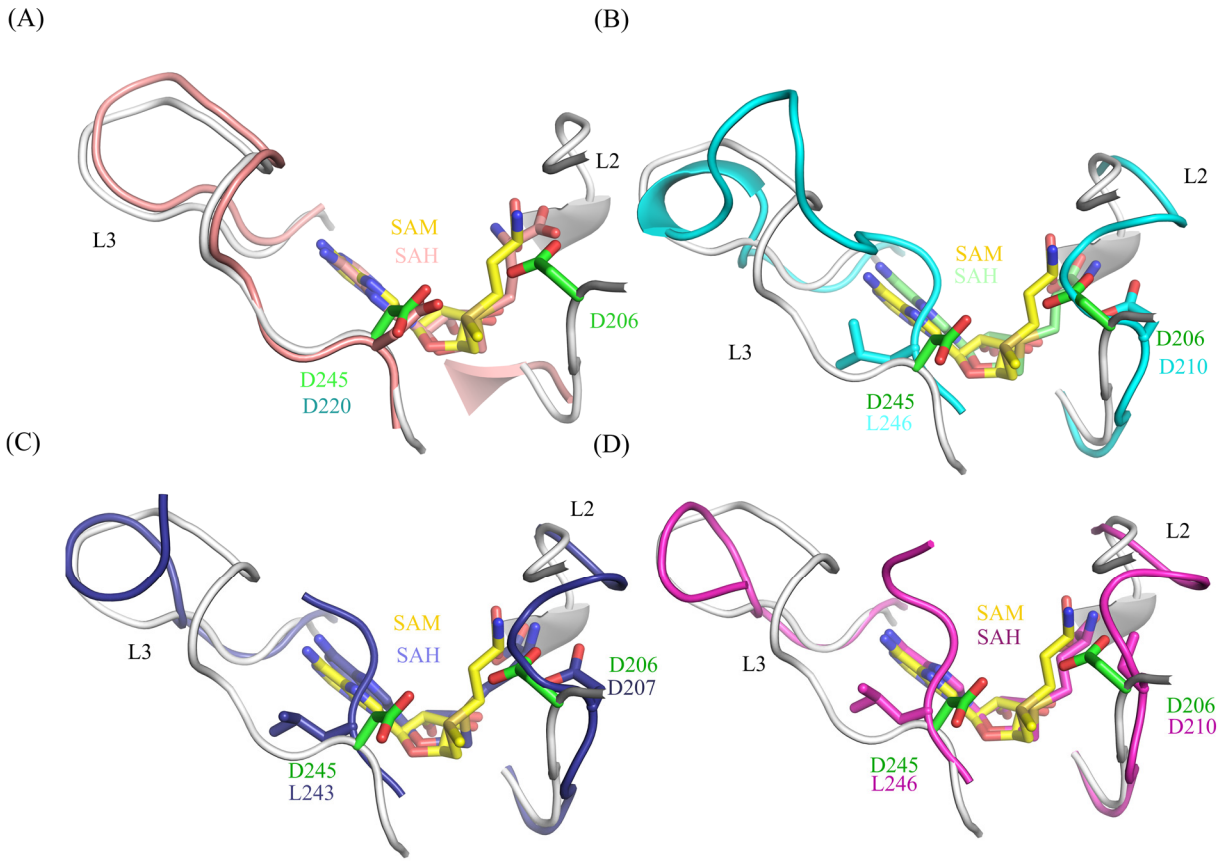

Figure S7. Conformational plasticity of the L2 and L3 active site loops in Trm10 orthologues. (**A**) Superposition of $_{Tk}$SPOUT_SAM (grey) with the SAH-bound SPOUT domain of $_{Sa}$Trm10 (light red, PDB 5a7y). Note that the L2 region is missing in the $_{Sa}$Trm10 structure bound to SAH. (**B**) Superposition of $_{Tk}$SPOUT_SAM (grey) with the SAH-bound SPOUT domain of $_{Sc}$Trm10 (cyan, PDB 4jwj). (**C**) Superposition of $_{Tk}$SPOUT_SAM (grey) with the SAH-bound SPOUT domain of $_{Sp}$Trm10 (blue, PDB 4jwh). (**D**) Superposition of $_{Tk}$SPOUT_SAM (grey) with the SAH-bound SPOUT domain of *Human* TrmT10A (magenta, PDB 4fmw). Note that D206 is highly conserved in all the Trm10 orthologues, while D245 is only present in $_{Tk}$Trm10 and $_{Sa}$Trm10.

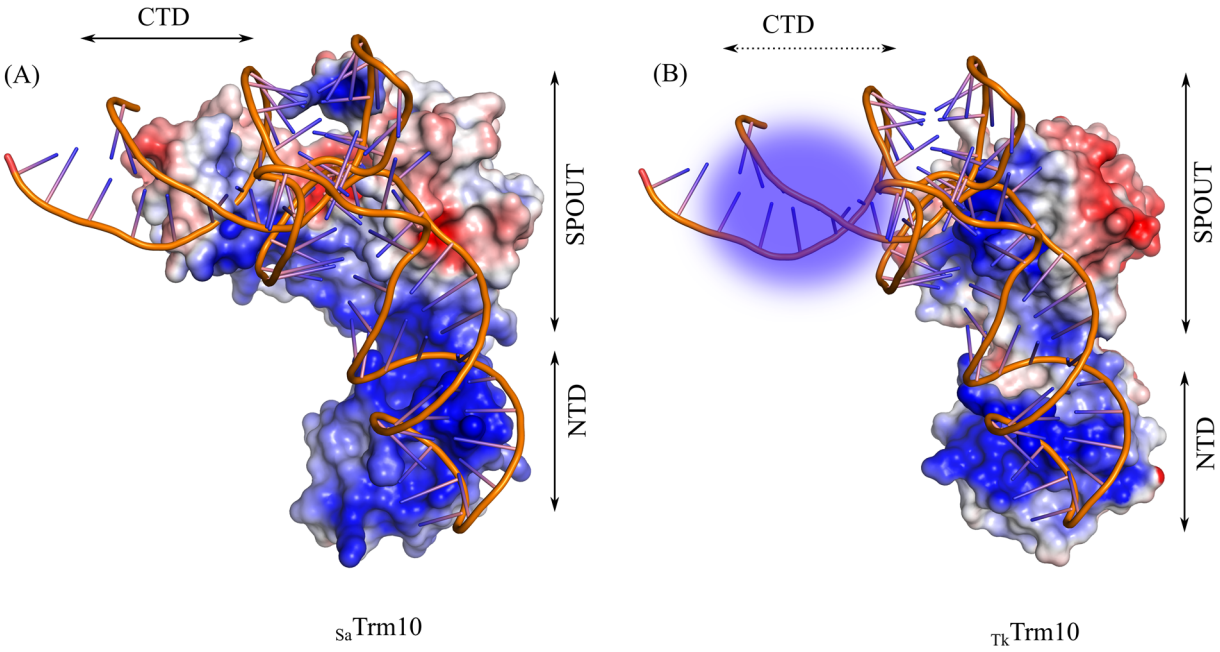

Figure S8. The electrostatic potential surface of $_{Tk}$Trm10Δ26 and comparison with $_{Sa}$Trm10 proposes a potential binding mode of substrate tRNA onto $_{Tk}$Trm10. (**A**) Docking model of $tRNA_i^{Met}$ onto $_{Sa}$Trm10, as proposed in Van Laer et al., 2016 (Van Laer *et al.*, 2016). (**B**) Placement of the tRNA onto the $_{Tk}$Trm10Δ26 structure in a similar position as in the $_{Sa}$Trm10-tRNA docking model shows a good superposition onto the positive charged surface of $_{Tk}$Trm10Δ26. Note that the C-terminal domain of $_{Tk}$Trm10 was not visible in the crystal structure.

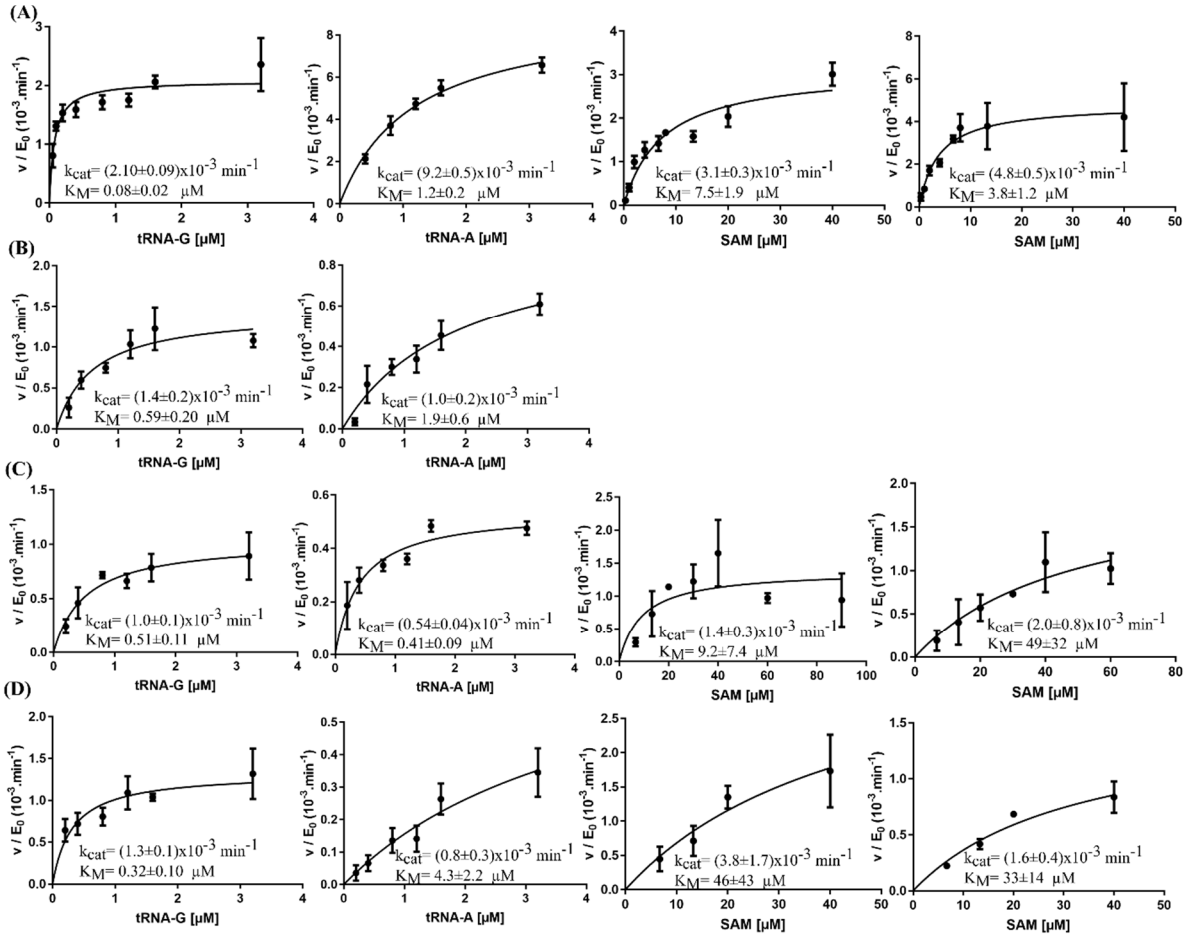

Figure S9: Steady state (Michaelis-Menten) kinetics of the methyltransferase reaction catalyzed by $_{Tk}$Trm10 mutants D245N (A), D245A (B), D206N (C) and D206N/D245N (D). From left to right curves are shown using either SAM at a fixed concentration of 20 µM and varying concentrations of tRNA-G or tRNA-A, or using SAM as a variable substrate at a fixed concentration (4 µM) of tRNA-G or tRNA-A. For the D245A mutant only full kinetic data with both tRNA's as variable substrates were obtained. Each data point is the average (± s.e.m.) of three independent measurements, except for D245N and D206N with SAM as variable substrate, where two independent measurements were performed. The k_{cat} and K_M values (± s.e.) resulting from fitting on the Michaelis-Menten equation are given in the insets.

References

Van Laer, B. *et al.* (2016) ‘Structural and functional insights into tRNA binding and adenosine N1-methylation by an archaeal Trm10 homologue’, *Nucleic Acids Research*. Oxford University Press, 44(2), pp. 940–953. doi: 10.1093/nar/gkv1369.